Sains Malaysiana 46(10)(2017): 1923–1933
*http://dx.doi.org/10.17576/jsm-2017-4610-31*

# The Influence of Geometrical Shapes of Stenosis on the Blood Flow in Stenosed Artery

(Pengaruh Bentuk Geometri Stenosis ke atas Aliran Darah dalam Arteri Stenos)

SARFARAZ KAMANGAR*, IRFAN ANJUM BADRUDDIN, N. AMEER AHAMAD, KALIMUTHU GOVINDARAJU, N. NIK-GHAZALI, N.J. SALMAN AHMED, A. BADARUDIN & T.M. YUNUS KHAN

ABSTRACT

*The present work was carried out to investigate the blood flow behavior and the severity of blockage caused in the arterial passage due to the different geometries such as elliptical, trapezium and triangular shapes of stenosis. The study was conducted with respect to various sizes of stenosis in terms of 70%, 80% and 90% area blockage of the arterial blood flow. The study was carried out numerically with the help of advance computational fluid dynamic software. It was found that the shape of the stenosis plays an important role in overall pressure drop across the blockage region of artery. The highest level of pressure drop was observed for trapezoidal shape of stenosis followed by elliptical and then by triangular shaped stenosis. The wall shear stress across the stenosis is great for trapezoidal shape followed by triangular and elliptical stenosis for same blockage area in the artery.*

*Keywords: CFD; coronary artery; non-Newtonian flow; stenosis*

ABSTRAK

*Kajian ini dijalankan untuk mengkaji sifat aliran darah dan keterukan laluan arteri yang tersumbat disebabkan oleh geometri stenosis yang berbeza seperti elips, trapezium dan bentuk segi tiga. Kajian ini dijalankan dengan pelbagai saiz stenosis pada kadar saiz sumbatan laluan arteri 70%, 80% dan 90%. Kajian ini dijalankan dengan kaedah berangka menggunakan perisian dinamik bendalir. Hasil kajian mendapati bahawa bentuk stenosis memainkan peranan penting dalam penurunan tekanan keseluruhan pada kawasan arteri yang tersumbat. Tahap tertinggi kejatuhan tekanan diperhatikan berlaku pada stenosis yang berbentuk trapezoid diikuti oleh elips dan kemudian oleh stenosis berbentuk segi tiga. Tegasan ricih permukaan seluruh stenosis yang paling besar adalah untuk bentuk trapezoid, diikuti oleh stenosis segi tiga dan elips.*

*Kata kunci: Aliran bukan Newtonian; arteri koronari; stenosis; CFD*

## INTRODUCTION

The development of atherosclerotic plaque on the inner side of the wall of arteries causes the myocardial infraction which is one of the most widespread diseases in human causing millions of deaths around the globe each year. The atherosclerotic plaque brings the most effective changes in the pressure, velocity, wall shear stress and impedance (flow resistance). The flow patterns such as velocity, pressure, directions strongly influenced by the geometry of the stenosis formed. It is more complex to assess the physiological severity of an intermediate stenosis in a single vessel or branched vessel using usual coronary angiogram or multi slice computed tomography (Tobis et al. 2007). There are a number of investigators such as Fatemi and Rittgers (1994), Giddens et al. (1976), Khalifa and Giddens (1978), Lee (1994) and O'Brien and Ehrlich (1985) who have reported that the flow pattern disturbance is a sensitive indicator of mild to moderate stenosis. It is known that the shape and dimension of stenosis play an important role in deciding the flow behavior in the cylindrical rigid artery as demonstrated by Lorenzini and Casalena (2008) that the trapezium plaques shape geometries are the most sever pathologies as they favor higher stain and further more chances of depositions on the walls of artery. The wall shear stress plays a vital role in the progression and development of arterial diseases was demonstrated by Fry (1973). The blood behavior inside the arteries have been subject of differing opinion as many researchers such as Deshpande et al. (1976) and Young (1968) have considered blood as Newtonian fluid for steady analysis through stenosed artery, whereas Shukla et al. (1980) and Misra and Shit (2006) considered the generalized model of Non-Newtonian fluid and analyzed the blood as a Casson and Herschel-Bulkley fluid. The pulsatile blood flow in the curved artery with varying degree of stenosis was analyzed by Ha and Lee (2014), Keshavarz et al. (2011), Liu (2007) as well as Paul and Larman (2009) who have investigated the effect of spiral blood flow in stenosed artery.

Although a significant amount of work has been carried out to investigate the blood flow in stenotic arteries in the past few decades, but not much work has been

reported on the blood flow across different shapes and sizes of stenosis in the arteries. Thus the current work was motivated to investigate the effect of different shapes of stenosis on the blood flow in the various percentage of area stenosis.

## METHODS

### STENOSIS GEOMETRY

There are a number of clinical and previously published data (Berglund et al. 1997; Lorenzini & Caselena 2008; Moser et al. 2000; Tang et al. 2003) which showed that stenosis does not have particular shapes. However, there are substantial evidences that the coronary artery area stenosis in the range of 70% to 90% blockage needs special attention since it may cause significant changes in the flow behavior and may lead to fatal conditions. Therefore, in order to study the effect of different shapes of stenosis on the flow behavior, the size of the stenosis is varied in 3 steps such as 70% (moderate), 80% (intermediate) and 90% (severe) area stenosis (AS). The blood flow behavior is investigated due to formation of stenosis in 3 different shapes namely, elliptical, trapezium and triangular. Figure 1 represents the different shapes of stenosis considered in the current study. The diameter of the artery is 3mm and the stenosis length has been fixed to 10mm in all models. Table 1 shows the dimensions used for the triangle and trapezium to develop the models of stenosis considered in the current study. The trapezoidal model in current study is based on the clinical study conducted on the group of patients by Back and Denton (1992), Roy et al. (2005) and Wilson et al. (1988). There are many studies in which the shape of stenosis was considered as elliptical in a patient specific coronary artery (Chaichana et al. 2013, 2012; Govindaraju et al. 2016a; Kamangar et al. 2017a, 2014; Ryou et al. 2012). The elliptical shape stenosis model was developed by using (1) (Dash et al. 1999).

$$\frac{\tilde{\eta}(\tilde{z})}{a} = 1 - \frac{h}{a}\sin\pi\left(\frac{\tilde{z}-d}{L}\right), \quad d \le \tilde{z} \le d + L, \tag{1}$$

where $\tilde{\eta}(\tilde{z})$ is the radius of stenosis, a, is the radius of an artery, $(\tilde{z})$ is along the axis of the artery and h is the maximum projection of the stenosis into the lumen.

$$\text{Area stenosis (AS)}\% = \frac{(\pi \times a^2) - [\pi \times (a-h)^2]}{\pi \times a^2}. \tag{2}$$

### COMPUTATIONAL MODELLING

Blood is assumed to be non-Newtonian, incompressible and governed by the Naiver-Stokes (3),

$$\rho\left(\frac{\partial v}{\partial t} + v.\nabla v\right) = \nabla.\tau - \nabla P. \tag{3}$$

The continuity equation for incompressible flow is:

$$\nabla.v = 0. \tag{4}$$

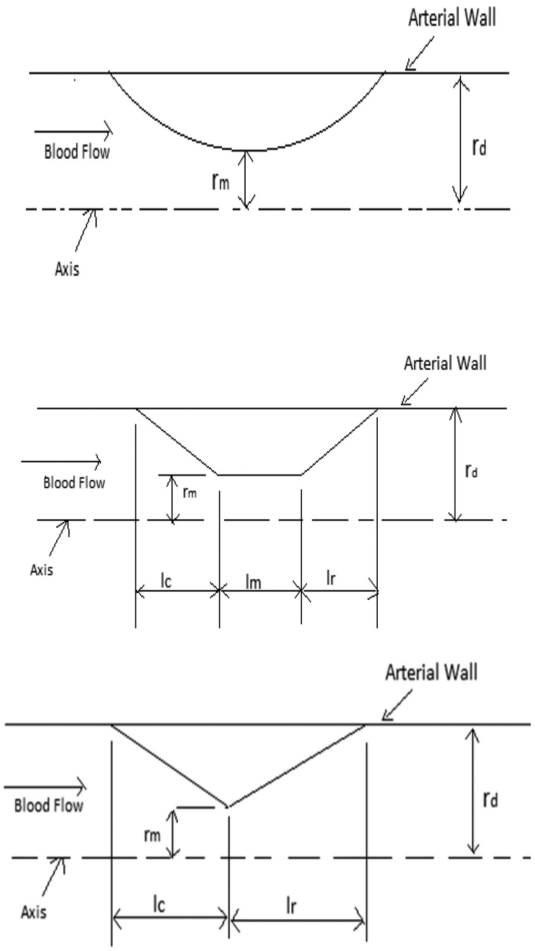


FIGURE 1. Schematic diagram for elliptical, trapezium and triangular stenosis geometry

Here $v$ = three-dimensional velocity vector, $t$ = time, $\rho$ = blood density, $P$ = pressure and $\tau$ = stress tensor

The governing equation for the non- Newtonian and Carreau model given by

$$\mu = \mu_\infty + (\mu_0 - \mu_\infty)[1 + (\lambda\gamma)^2]^{(n-1)/2}, \tag{5}$$

where $\lambda$ (time constant) = 3.313s; $n$(power law index) = 0.3568, $\mu_0$ (low shear viscosity) = 0.56$P$, $\mu_\infty$ (high shear viscosity) = 0.0345P and the density of the blood $(\rho)$ is assumed as 1050 kg/m$^3$ (Govindaraju et al. 2014; Peelukhana et al. 2009). Finite volume software ANSYS CFX 14.5 (ANSYS Inc) was used for flow simulations.

### BOUNDARY CONDITIONS

In order to ensure the realistic physiological conditions, the 3D numerical simulation was considered with a transient Pulsatile pressure p(t) (Figure 2(a)) at the inlet and transient parabolic velocity u(t) at the outlet (Figure 2(b)) (Konala et al. 2011) with no slip condition at the arterial wall. The same inlet and outlet boundary conditions were used to solve all the models. The mean hyperemic flow rate $(\tilde{Q})$ 175, 165 and 115 mL/min was used to acquire the velocity

TABLE 1. Dimensions of different stenosis shapes (All the dimension are in mm)

| Area stenosis (AS) | $r_d$ | $r_m$ | Triangle | | | Elliptical | | | Trapezium | | |
|---|---|---|---|---|---|---|---|---|---|---|---|
| | | | $l_c$ | $l_m$ | $l_r$ | lc | $l_m$ | $l_r$ | $l_c$ | $l_m$ | $l_r$ |
| 70% | 1.5 | 0.82 | 5 | - | 5 | - | - | - | 3.5 | 3 | 3.5 |
| 80% | 1.5 | 0.67 | 5 | - | 5 | - | - | - | 3.5 | 3 | 3.5 |
| 90% | 1.5 | 0.47 | 5 | - | 5 | - | - | - | 3.5 | 3 | 3.5 |

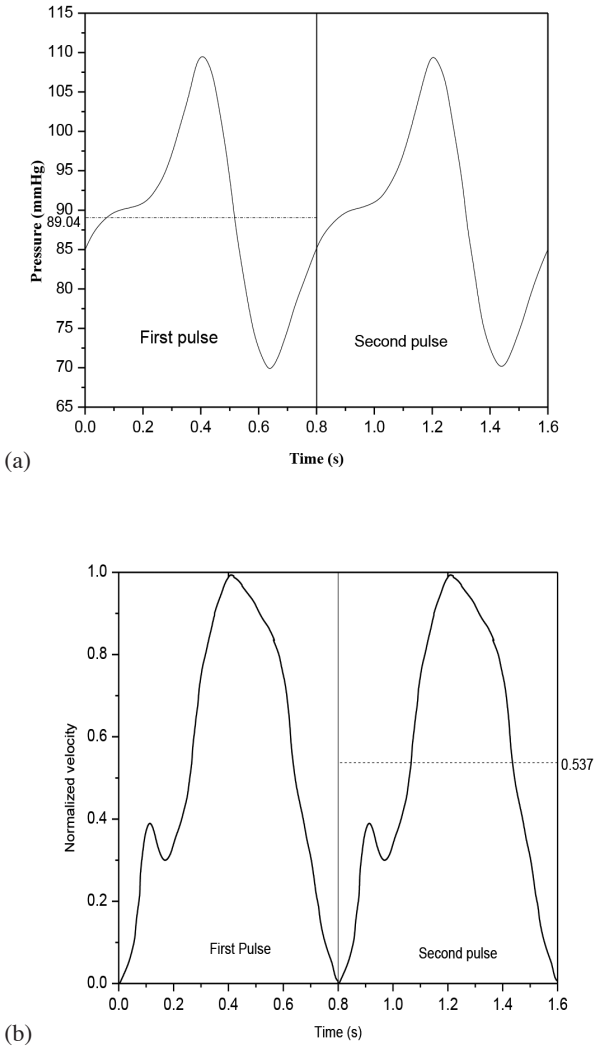


FIGURE 2. (a) Time varying physiological pressure applied at the inlet and (b) coronary flow wave form $\overline{u}/\overline{u}_{p-t}$ versus $t$ applied at the outlet (Banerjee et al. 2003; Roy et al. 2006)

profile for 70%, 80% and 90% AS, respectively (Konala et al. 2011). The shear stress transport (SST) turbulence model belonging to k-ω model was used for modelling the flow which gives the accurate and robust results for high Reynolds number as noted by Jozwik and Obidowski (2010), and Kagadis et al. (2008). The uncertainty in shear layer could be possible during the hypermic flow conditions because of disturbances in the cardiac cycle and irregularities in the different shapes of stenosis (Banerjee et al. 2013; Mallinger & Drikakis 2002; Rajabi-Jagharghet al. 2011).

Initially, steady-state flow analysis was performed. This was followed by transient flow analysis considering the results from the steady-state analysis as the initial guess in CFD simulation.

For the steady state analysis, the following values of parameters at the inlet and outlet were taken, namely: mean physiologic pressure at the inlet: 89.04 mmHg; and mean velocity at the outlet: 0.413, 0.389 and 0.271 m/s correspond to 70%, 80% and 90% AS (Govindaraju et al. 2016b).

## METHODS

The 3D computational domain was initially meshed with hexahedral elements in the range of 250,000 and 5,00,000 for 70%, 80% and 90% AS for all the three different shapes of models. The commercially available software CFX 14.5 (ANSYS CFX, 14.5 Canonsburg, PA) was employed for blood flow simulation (Kamangar et al. 2017b). Figure 3 shows the discretized domain for the trapezoidal model with 80%AS. The fine grid structure of 368,244 tetrahedral elements was generated. The grid dependent study was carried out to highlight that the above-mentioned 368,244 elements are right choice of mesh size for this particular study. Details of mesh independent study are shown in Table 2 and Figure 4. The transient flow analysis was run for 640 time steps (0.005 s per time step) representing 4 cycles (0.8 s each) of pulsatile flow with each time step converging to a residual target of $1\times10^{-5}$.

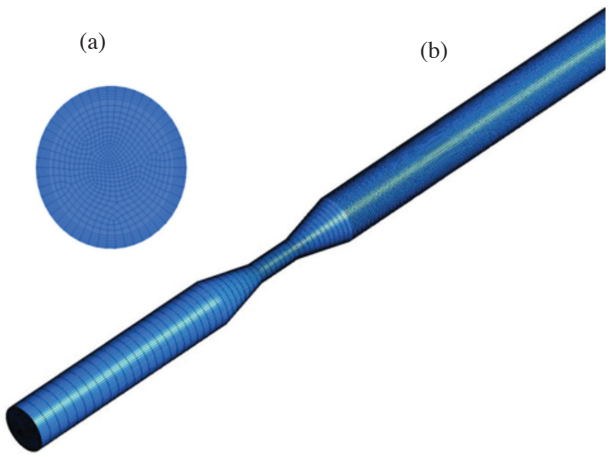


FIGURE 3. Computational meshes used for numerical study in the trapezoidal model for 80%AS (a) front view and (b) isometric view

TABLE 2. Mesh-independent study for 80% AS trapezoidal model

| 80%AS trapezoidal model | No. of elements | Max pressure drop (mmHg) | Difference (mmHg) | Times in H:min:s |
|---|---|---|---|---|
| Mesh 1 | 265825 | 20.5388 | - | 3:38:34 |
| Mesh 2 | 368244 | 20.9187 | 0.379 | 4:23:55 |
| Mesh 3 | 507608 | 21.1073 | 0.188 | 6:46:38 |

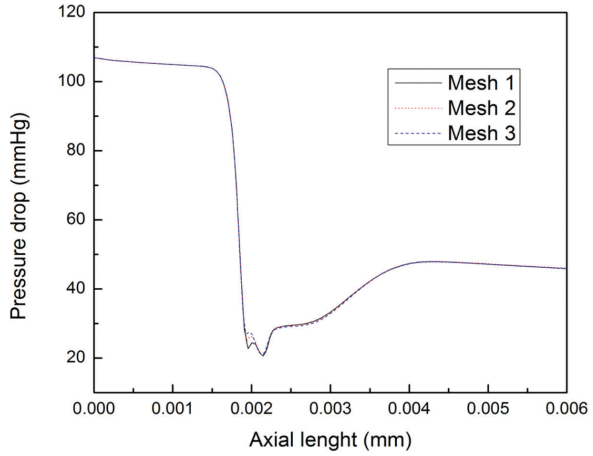


FIGURE 4. Comparison of mesh-independent study for various numbers of elements during the peak systole

The current study was carried out for the hyperemic flow rates, therefore to validate the current methods a steady state simulation for the flow rates of 50 and 100 mL/min was performed. The numeric results obtained was compared with the closely related articles previously published in the open literature (Banerjee et al. 2003). It can be observed clearly from Figure 5 that the axial pressure drop for the flow rate of 50 and 100 mL/min is almost close. Therefore, the results are found to be good agreement with the previous published article.

## RESULTS AND DISCUSSION

Figures 6, 7 and 8 show the comparison of radial velocity for the various shapes of stenosis models in 70%, 80% and 90% AS during the cardiac cycle. As expected, the velocity profile is higher for systolic as compared to the diastolic period of cardiac cycle in all the models. It is observed that the blood velocity for the different shapes of stenosis does not vary much for proximal (2 mm before stenosis) position during the cardiac cycle. Whereas, the velocity is increased as percentage area stenosis increased. The highest velocity is found for the 90%AS stenosis models. It was also observed that the maximum velocity is found at the throat (mid of the stenosis) sections. It is noted that the trapezoidal shape of stenosis has the maximum velocity followed by the elliptical and triangular shape of the stenosis. Similarly, the velocity is maximum for the trapezoidal model as compared to the other two models

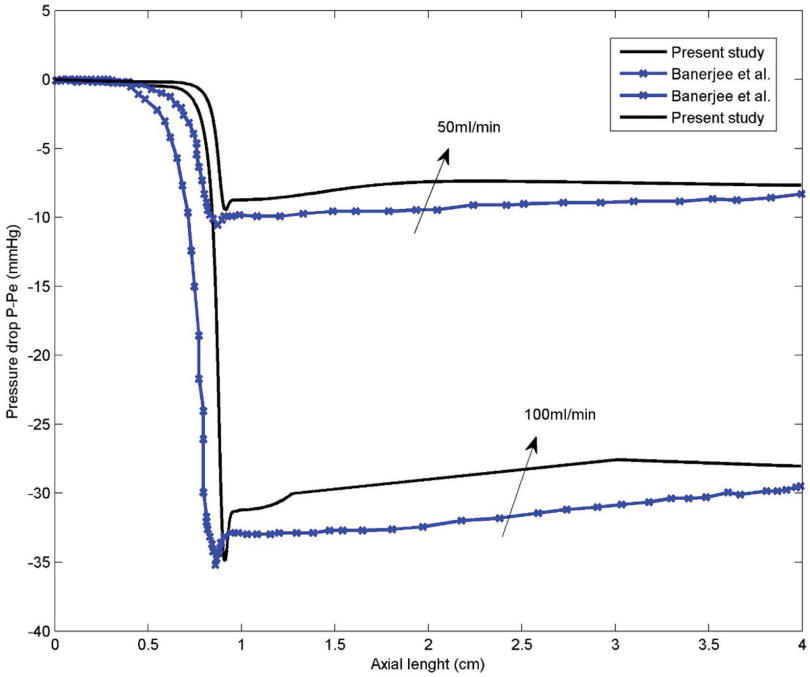


FIGURE 5. Comparison of present study with previous published data of Banerjee et al. 2003

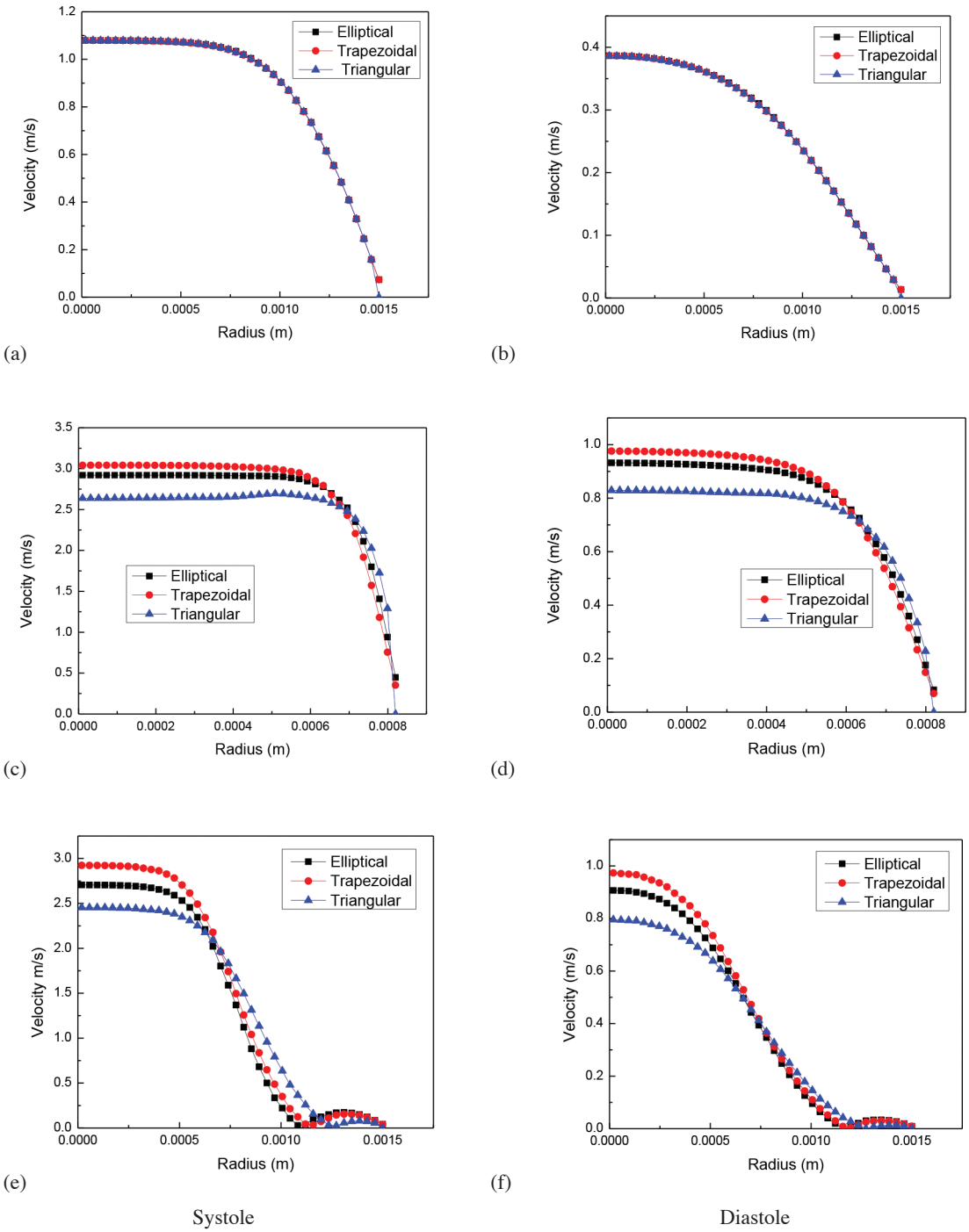


FIGURE 6. Velocity profile for various shapes of stenosis in 70%AS during the systole and diastole period of cardiac cycle: (a) and (b) proximal, (c) and (d) mid of stenosis and (e) and (f) distal

across the distal (2 mm after the stenosis) section. The maximum velocity was observed for the trapezium model as compared to the elliptical and triangular models during the diastolic period of cardiac cycle.

The pressure drop developed due to the presence of stenosis is very important parameter to understand the severity of blockage that may lead to fatal situation if not diagnosed and measured accurately. It is well known that the doctors in under developed countries rely heavily on angiographic images to make decision about severity of stenosis where %AS is considered as deciding parameter without giving much attention to the geometry of stenosis. The pressure drop across the length of artery at various pulse time and geometry of stenosis is shown in Figure 9. The pressure drops suddenly when blood flow encounters stenosis and then starts recovering after having passed through the blockage area. As expected, the preserve drop across stenosis increases substantially when %AS

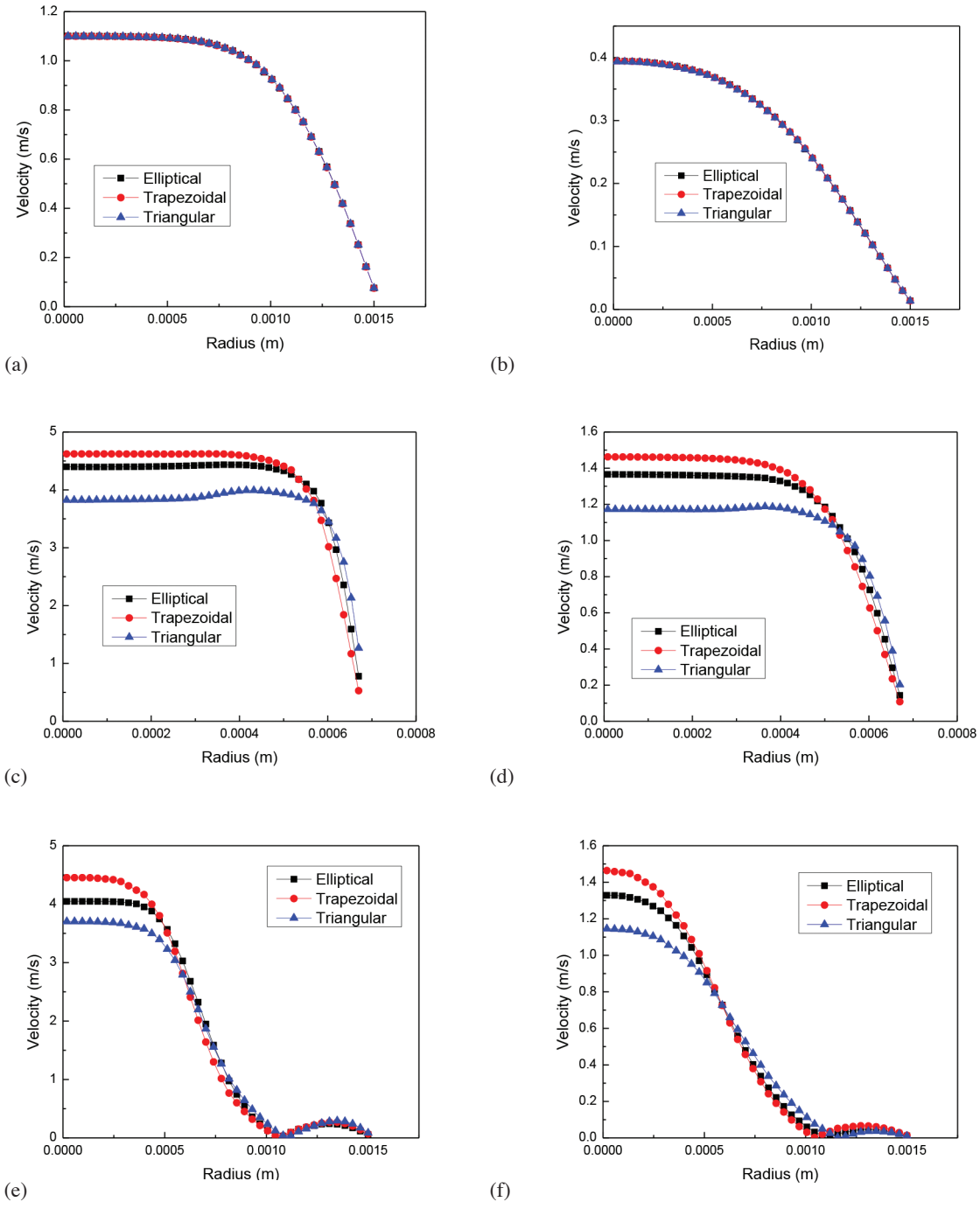


FIGURE 7. Velocity profile for various shapes of stenosis in 80%AS during the systole and diastole period of cardiac cycle: (a) and (b) proximal, (c) and (d) mid of stenosis and (e) and (f) distal

increases. It is evident from Figure 9 that the pressure drops around 3 times for elliptical stenosis when %AS increases from 70% to 90%, which represents a severe condition for patient. It is obvious from Figure 9 that the shape of stenosis has significant effect on pressure drop since trapezoidal stenosis produces substantial higher drop in pressure as compared to elliptical stenosis which in turn is higher than that of triangular shape stenosis. For instance, the pressure drop across elliptical stenosis for 90% AS is 20 mmHg greater than triangular stenosis and trapezoidal shape gives 27 mmHg higher pressure drop than that of elliptical shape for same %AS. This is substantial variation of pressure drop when geometry of stenosis changes thus the geometry of blockage area cannot be ignored while evaluating the severity of the stenosis.

Figure 10 shows the overall transient pressure drop $\Delta\tilde{p} = P_a\text{-}P_r$ (where $P_a$ is the pressure measured at 3 mm proximal to the start of converging portion and $P_r$ is the

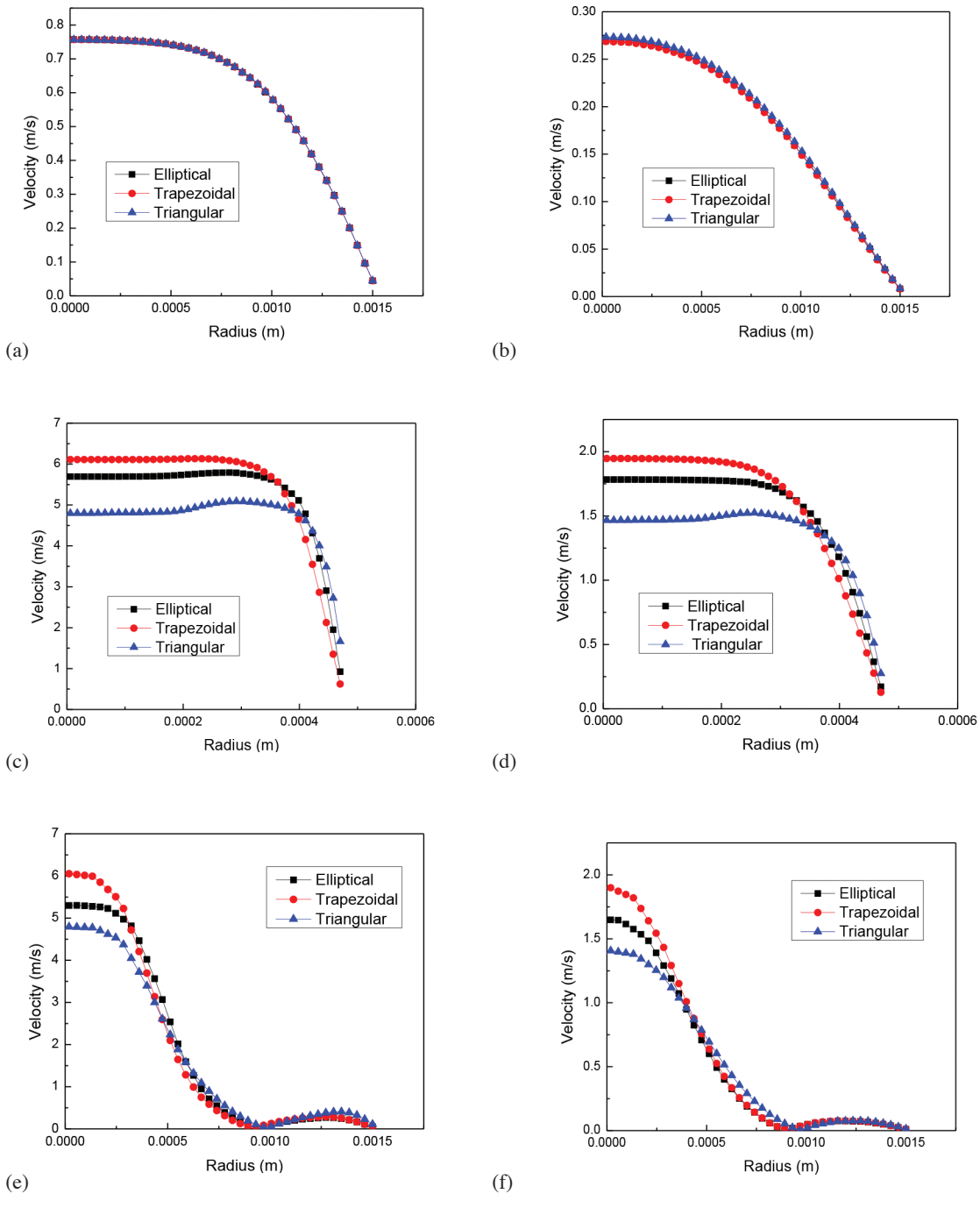


FIGURE 8. Velocity profile for various shapes of stenosis in 90%AS during the systole and diastole period of cardiac cycle: (a) and (b) proximal, (c) and (d) mid of stenosis and (e) and (f) distal

distal recovery pressure) which was taken during the third and fourth cycles for the stenosis. The mean pressure drop by integrating over the cardiac cycle shown by the horizontal dash line in Figure 10, were -12.6, -15.7 and -19.8 mmHg for the triangular, elliptical and trapezoidal shapes of stenosis. The previously mentioned mean pressure drop values further emphasis that the trapezoidal shaped stenosis poses a significant higher risk to the patient as compared to the other two geometries.

Figure 11 shows the stress at the arterial wall which is the indication of health of arterial wall in the long run. The stress at the wall around stenosis area is much higher than the other areas and the stress increases with increase in the blockage area. It is found that the arterial wall has to endure much higher stresses due to trapezoidal stenosis as compared to that of triangular stenosis and elliptical shape produces smallest wall stress of the three geometries of stenosis being investigated. Thus it can be conveniently

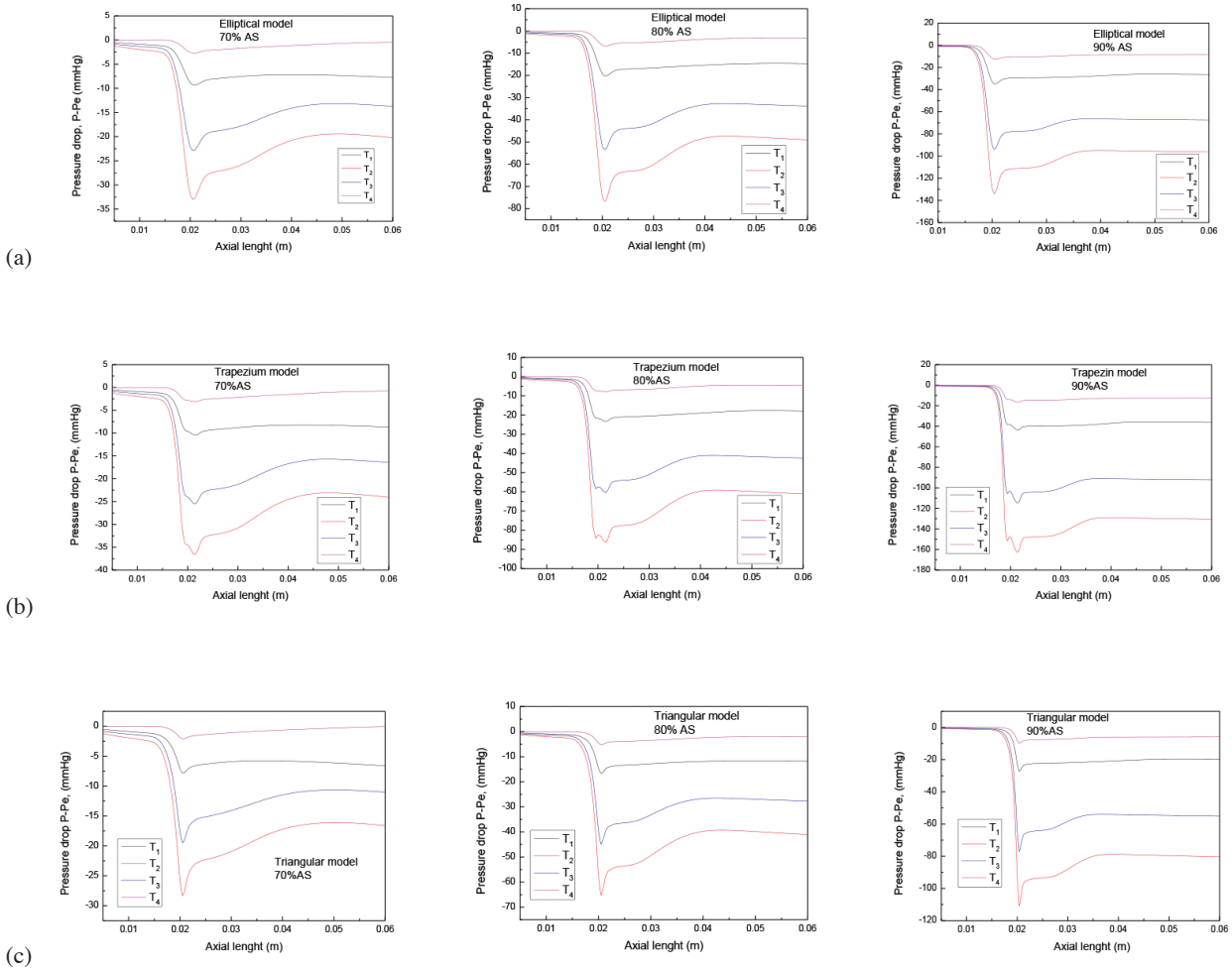


FIGURE 9. Axial pressure drop *P-Pe*, along the stenosis at various time at hyperemia for (a) elliptical, (b) trapezium and (c) triangular model in 70%, 80%, and 90%AS

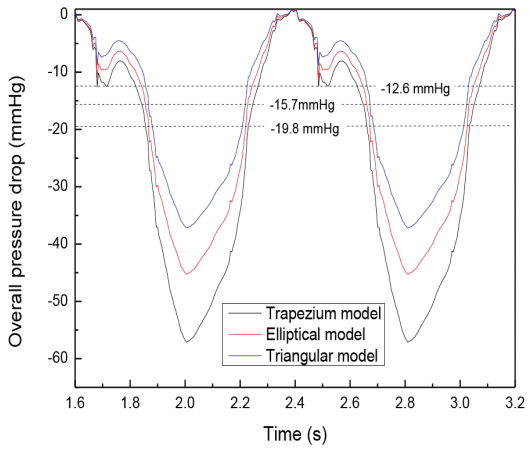


FIGURE 10. Overall pressure drop $\tilde{p}$ across the different shapes of stenosis (trapezium, elliptical and triangular) during the cardiac cycle at hypermic flow in 80%AS

said that the chances of arterial wall rupture due to stenosis formation are highest in trapezoidal shape followed by triangular and elliptical stenosis shape.

## CONCLUSION

The findings of current work can be summarized as follows: The increase in percentage area stenosis, increase

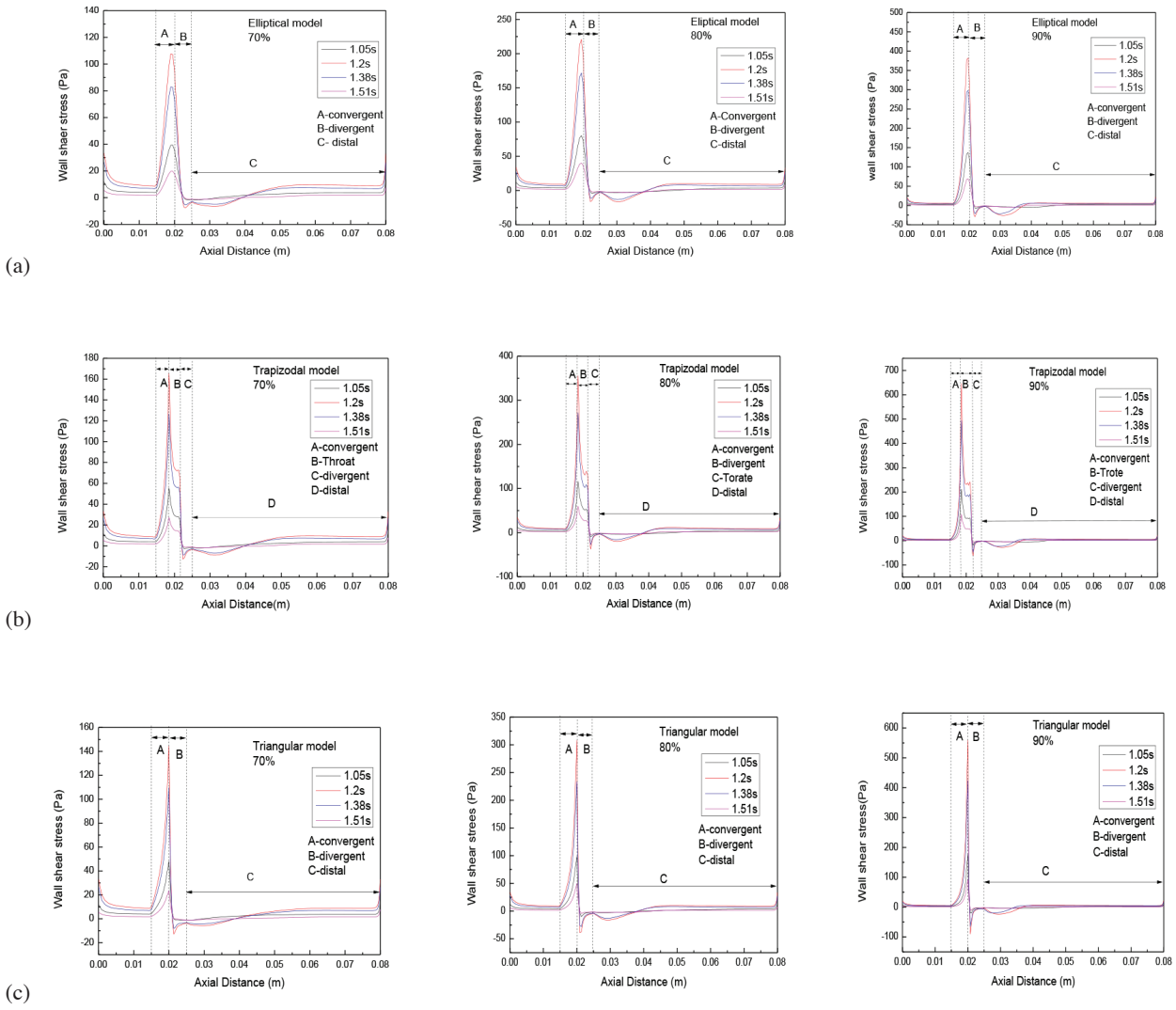


FIGURE 11. Wall shear stress along the artery at various time steps during the cardiac cycle

the velocity profile inside the blockage region. The shape of stenosis has significant effect on the flow characteristics leading to varied diagnostics parameters such as pressure drop across the blockage area. The pressure drop is highest in case of trapezoidal stenosis and least for triangular shape for same area blockage due to stenosis thus the severity level of patients increases in case of trapezoidal geometry. The arterial wall is more prone to rupture due to trapezoidal stenosis than the elliptical or triangular shapes.

## ACKNOWLEDGEMENTS

The authors would like to thank University of Malaya for funding the project under Grant No. PG212-2015B and PG203-2015B.

## REFERENCES

Banerjee, R.K., Back, L.H., Back, M.R. & Cho, Y.I. 2003. Physiological flow analysis in significant human coronary artery stenoses. *Biorheology* 40(4): 451-476.

Berglund, H., Luo, H., Nishioka, T., Fishbein, M.C., Eigler, N.L., Tabak, S.W. & Siegel, R.J. 1997. Highly localized arterial remodeling in patients with coronary atherosclerosis. *Circulation* 96(5): 1470-1476.

Chaichana, T., Sun, Z. & Jewkes, J. 2012. Computational fluid dynamics analysis of the effect of plaques in the left coronary artery. *Computational and Mathematical Methods in Medicine* 2012: Article ID. 504367.

Chaichana, T., Sun, Z. & Jewkes, J. 2013. Haemodynamic analysis of the effect of different types of plaques in the left coronary artery. *Computerized Medical Imaging and Graphics* 37(3): 197-206.

Chaichana, T., Sun, Z. & Jewkes, J. 2014. Impact of plaques in the left coronary artery on wall shear stress and pressure gradient in coronary side branches. *Computer Methods in Biomechanics and Biomedical Engineering* 17(2): 108-118.

Dash, R.K., Jayaraman, G. & Mehta, K.N. 1999. Flow in a catheterized curved artery with stenosis. *Journal of Biomechanics* 32(1): 49-61.

Deshpande, M.D., Giddens, D.P. & Mabon, R.F. 1976. Steady laminar flow through modelled vascular stenoses. *Journal of Biomechanics* 9(4): 165-174.

Fatemi, R.S. & Rittgers, S.E. 1994. Derivation of shear rates from near-wall LDA measurements under steady and pulsatile flow conditions. *Transactions-American Society of Mechanical Engineers Journal of Biomechanical Engineering* 116: 361-361.

Fry, D.L. 1973. Responses of the arterial wall to certain physical factors. In *Ciba Foundation Symposium 12 - Atherogenesis: Initiating Factors*, edited by Porter, R. & Knight, J. John Chichester: Wiley & Sons, Ltd. doi: 10.1002/9780470719954.ch5.

Giddens, D.P., Mabon, R.F. & Cassanova, R.A. 1976. Measurements of disordered flows distal to subtotal vascular stenoses in the thoracic aortas of dogs. *Circulation Research* 39(1): 112-119.

Govindaraju, K., Badruddin, I.A., Viswanathan, G.N., Kamangar, S., Ahmed, N.S. & Al-Rashed, A.A. 2016a. Influence of variable bifurcation angulation and outflow boundary conditions in 3D finite element modelling of left coronary artery on coronary diagnostic parameter. *Current Science* 111(2): 368-374.

Govindaraju, K., Viswanathan, G.N., Badruddin, I.A., Kamangar, S., Ahmed, N.J. & Al-Rashed, A.A. 2016b. A parametric study of the effect of arterial wall curvature on non-invasive assessment of stenosis severity: Computational fluid dynamics study. *Current Science* 111(3): 483-491.

Govindaraju, K., Kamangar, S., Badruddin, I.A., Viswanathan, G.N., Badarudin, A. & Ahmed, N.S. 2014. Effect of porous media of the stenosed artery wall to the coronary physiological diagnostic parameter: a computational fluid dynamic analysis. *Atherosclerosis* 233(2): 630-635.

Ha, H. & Lee, S.J. 2014. Effect of swirling inlet condition on the flow field in a stenosed arterial vessel model. *Medical Engineering & Physics* 36(1): 119-128.

Jozwik, K. & Obidowski, D. 2010. Numerical simulations of the blood flow through vertebral arteries. *Journal of Biomechanics* 43(2): 177-185.

Kamangar, S., Badruddin, I.A., Badarudin, A., Nik-Ghazali, N., Govindaraju, K., Salman Ahmed, N.J. & Yunus Khan, T.M. 2017a. Influence of stenosis on hemodynamic parameters in the realistic left coronary artery under hyperemic conditions. *Computer Methods in Biomechanics and Biomedical Engineering* 20(4): 365-372.

Kamangar, S., Badruddin, I.A., Govindaraju, K., Nik-Ghazali, N., Badarudin, A., Viswanathan, G.N., Ahmed, N.S. & Khan, T.Y. 2017b. Patient-specific 3D hemodynamics modelling of left coronary artery under hyperemic conditions. *Medical & Biological Engineering & Computing* 111(2): 368-374.

Kamangar, S., Kalimuthu, G., Anjum Badruddin, I., Badarudin, A., Salman Ahmed, N.J. & Khan, T.M. 2014. Numerical investigation of the effect of stenosis geometry on the coronary diagnostic parameters. *The Scientific World Journal* 2014: Article ID 354946.

Kagadis, G.C., Skouras, E.D., Bourantas, G.C., Paraskeva, C.A., Katsanos, K., Karnabatidis, D. & Nikiforidis, G.C. 2008. Computational representation and hemodynamic characterization of *in vivo* acquired severe stenotic renal artery geometries using turbulence modeling. *Medical Engineering & Physics* 30(5): 647-660.

Keshavarz-Motamed, Z. & Kadem, L. 2011. 3D pulsatile flow in a curved tube with coexisting model of aortic stenosis and coarctation of the aorta. *Medical Engineering & Physics* 33(3): 315-324.

Khalifa, A.M.A. & Giddens, D.P. 1978. Analysis of disorder in pulsatile flows with application to poststenotic blood velocity measurement in dogs. *Journal of Biomechanics* 11(3): 129-141.

Konala, B.C., Das, A. & Banerjee, R.K. 2011. Influence of arterial wall-stenosis compliance on the coronary diagnostic parameters. *Journal of Biomechanics* 44(5): 842-847.

Lee, T.S. 1994. Steady laminar fluid flow through variable constrictions in vascular tube. *Journal of Fluids Engineering* 116(1): 66-71.

Liu, B. 2007. The influences of stenosis on the downstream flow pattern in curved arteries. *Medical Engineering & Physics* 29(8): 868-876.

Lorenzini, G. & Casalena, E. 2008. CFD analysis of pulsatile blood flow in an atherosclerotic human artery with eccentric plaques. *Journal of Biomechanics* 41(9): 1862-1870.

Mallinger, F. & Drikakis, D. 2002. Instability in three-dimensional, unsteady, stenotic flows. *International Journal of Heat and Fluid Flow* 23(5): 657-663.

Misra, J.C. & Shit, G.C. 2006. Blood flow through arteries in a pathological state: A theoretical study. *International Journal of Engineering Science* 44(10): 662-671.

Moser, K.W., Kutter, E.C., Georgiadis, J.G., Buckius, R.O., Morris, H.D. & Torczynski, J.R. 2000. Velocity measurements of flow through a step stenosis using magnetic resonance imaging. *Experiments in Fluids* 29(5): 438-447.

O'Brien, V. & Ehrlich, L.W. 1985. I. Simple pulsatile flow in an artery with a constriction. *Journal of Biomechanics* 18(2): 117-127.

Paul, M.C. & Larman, A. 2009. Investigation of spiral blood flow in a model of arterial stenosis. *Medical Engineering & Physics* 31(9): 1195-1203.

Peelukhana, S.V., Back, L.H. & Banerjee, R.K. 2009. Influence of coronary collateral flow on coronary diagnostic parameters: An *in vitro* study. *Journal of Biomechanics* 42(16): 2753-2759.

Rajabi-Jaghargh, E., Kolli, K.K., Back, L.H. & Banerjee, R.K. 2011. Effect of guidewire on contribution of loss due to momentum change and viscous loss to the translesional pressure drop across coronary artery stenosis: An analytical approach. *Biomedical Engineering Online* 10: 51.

Roy, A.S., Back, L.H. & Banerjee, R.K. 2006. Guidewire flow obstruction effect on pressure drop-flow relationship in moderate coronary artery stenosis. *Journal of Biomechanics* 39(5): 853-864.

Ryou, H.S., Kim, S., Kim, S.W. & Cho, S.W. 2012. Construction of healthy arteries using computed tomography and virtual histology intravascular ultrasound. *Journal of Biomechanics* 45(9): 1612-1618.

Shukla, J.B., Parihar, R.S. & Rao, B.R.P. 1980. Effects of stenosis on non-Newtonian flow of the blood in an artery. *Bulletin of Mathematical Biology* 42(3): 283-294.

Tang, D., Yang, C., Kobayashi, S., Zheng, J. & Vito, R.P. 2003. Effect of stenosis asymmetry on blood flow and artery compression: A three-dimensional fluid-structure interaction model. *Annals of Biomedical Engineering* 31(10): 1182-1193.

Tobis, J., Azarbal, B. & Slavin, L. 2007. Assessment of intermediate severity coronary lesions in the catheterization laboratory. *Journal of the American College of Cardiology* 49(8): 839-848.

Young, D.F. 1968. Effect of a time-dependent stenosis on flow through a tube. *Journal of Manufacturing Science and Engineering* 90(2): 248-254.

Sarfaraz Kamangar*, N. Nik-Ghazali & A. Badarudin
Department of Mechanical Engineering
University of Malaya
50603 Kuala Lumpur, Federal Territory
Malaysia

Irfan Anjum Badruddin
Department of Mechanical Engineering
College of Engineering
King Khalid University
Abha - 61421
Kingdom of Saudi Arabia

N. Ameer Ahamad
Mathematics Department, Faculty of Science
University of Tabuk
Saudi Arabia

Kalimuthu Govindaraju
Department of Mechanical and Industrial Engineering
Mekelle University, Mekelle
Ethiopia

N.J. Salman Ahmed
Department of Mechanical and Industrial Engineering
Sultan Qaboos University
33, Alkhoud, Muscat, 123
Oman

T.M. Yunus Khan
Department of Mechanical Engineering
CMR Technical Campus, Hyderabad
India

*Corresponding author; email: sarfaraz.kamangar@gmail.com

Received: 9 March 2016
Accepted: 20 March 2017